Neutron Physics

Emily P. Wang*
MIT Department of Physics
(Dated: November 11, 2004)

Thermal neutrons in a beam emerging from the MIT research reactor were used to study the Maxwell-Boltzmann distribution, the Bragg scattering of neutrons off the atomic planes of a copper crystal, the De Broglie relation, and the neutron absorption cross section. It was concluded that the De Broglie relation was observed for neutrons, and the temperature obtained for the reactor using the Maxwell Boltzmann distribution was $(64 \pm 19)^oC$, which compared well to the actual reactor core temperature of 50.8^oC. The $1/v$ dependency for Boron's transmission cross section was observed–the slope of the fitted line was $(1.48\times10^{-18}\pm3.4\times10^{-18})cm^3/s$, while the theoretical value was $(1.660 \times 10^{-22}cm^3/sec)$. The large error margin may have been caused by the uncertainty in determining the peak times for neutron pulses, insufficient time for data gathering, and insufficient number of θ_B observed.

1. INTRODUCTION

Investigations were done at the MIT Research Reactor (MITR), using a collimated beam of low-energy thermal neutrons emerging from the reactor. A nuclear reactor is analoguous in its function to a coal-powered fire, with the nuclear reactions serving as the "fuel" consumed by the reactor and the neutrons serving as the "heat" emitted by the reactor. Typically, $^{235}_{92}U$, a fissionable isotope of uranium, is used as the fuel in a reactor. Within the reactor, neutrons react with the uranium nuclei and split it into two smaller nuclei, in addition to other particles–neutrons, gamma-rays, electrons, and so on. The newly freed neutrons go on to react with more uranium nuclei, causing a chain reaction. Neutrons are typically moderated in a reactor–that is, they are slowed down in energy by scattering off of light atoms. By studying the moderated neutrons that are emitted, one can obtain a Maxwell-Boltzmann spectrum and thereby measure the temperature of the reactor's moderating agent (MITR uses normal water as a moderator). The velocity of neutrons can be obtained using time-of-flight spectroscopy. In addition, the wave-particle duality of particles can be studied by using neutrons from the beam and placing regular crystals in the pathway of the beam.

The wave-particle duality of matter was a problem that physicists were dealing with at the beginning of the 21st century. There was evidence that the electromagnetic field behaved both like a wave and particle in its interactions with matter. Experiments such as Young's double-slit interference experiments in 1801, Hertz's experiments with radio waves in 1887, and von Laue's discovery of X-ray diffraction in 1912 allowed physicists to measure the wavelength of electromagnetic radiation ranging from radio to X-rays. Concepts that highlighted the particle-like nature of the electromagnetic field were Planck's theory of the black-body spectrum and Einstein's theory of the photoelectric effect, both of which showed that electromagnetic radiation is absorbed at a surface in quantized packets of energy, not as a continuous flow. [1]

An experiment which showed electromagnetic radiation behaved both like a wave and a particle was Compton scattering, where an X-ray of wavelength λ interacted with free electrons like particles with energy hc/λ. De-Broglie hypothesized in 1924 that all matter should show this wave-particle duality, and this composite picture was eventually accepted by physicists. Confirmation for the De Broglie relation came with the discovery of electron diffraction in 1927. This was followed by the demonstration that diffraction occurred with other particles, such as alpha particles. Bragg formulated a law that explained these results, envisioning the crystal lattice as a series of atomic planes and describing the preferred directions for constructive interference of a beam of radiation incident upon these crystal planes [2]. The observations of crystal diffraction has allowed physicists to to probe the structure of crystals and use X-ray spectroscopy. [3]

Another property that can be investigated using the neutron beam from a nuclear reactor is the transmission cross section of various materials. If different absorbers are put into the pathway of the neutron beam of the reactor, the attenuated intensity can be measured and compared to the nonattenuated intensity, allowing calculation of the transmission cross section of the absorber. The absorber used in this experiment was a Boron-containing Pyrex glass, whose transmission cross section exhibited a $1/v$ dependency.

2. DE BROGLIE AND WAVE-PARTICLE DUALITY

The De Broglie relation for matter is:

$$\lambda = \frac{h}{mv} \tag{1}$$

where λ = the De Broglie wavelength and h = Planck's constant. This relation can also be applied to photons–in this case, $E = h\nu$ and $p = E/c$. [1]

*Electronic address: wangfire@mit.edu

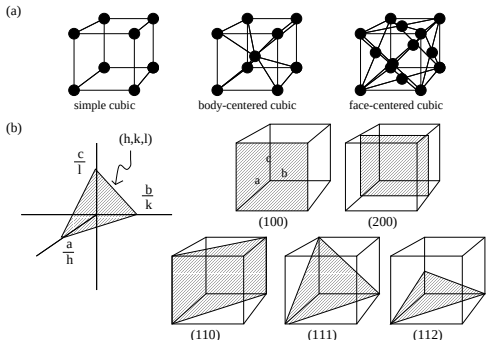

FIG. 1: (a) Different atomic packing forms of cubic crystals. (b) Diagrams of Miller indices used to describe different atomic planes in a crystal.

3. SCATTERING OF RADIATION

Generally speaking, a three-dimensional grating will not diffract a parallel beam of monochromatic light and will instead behave like a transparent medium. For any given wavelength λ, however, there will be certain preferred directions θ_B where constructive interference of the diffracted rays will occur. Likewise, given a direction of incidence for light, there are certain values of λ that will yield constructive interference. [3] This experiment does the latter–setting the diffracting copper crystal at specific orientations, we selected out the specific wavelengths of neutron radiation that satisfied the criteria for constructive interference.

Bragg's Diffraction Law describes the relation between λ and θ_B as follows:

$$2dsin\theta_B = n\lambda \tag{2}$$

where θ_B is the angle of incidence, which is equal to the angle of reflection, d is the interplanar spacing, and λ is the wavelength of the radiation. [2]

This equation is similar to that given for the one-dimensional scattering of radiation, for instance, the scattering of radiation from a transmission grating. The key difference is that the angles of incident and exiting radiation from the crystal are both equal to θ_B in the case of three-dimensional Bragg scattering, while in the case of one-dimensional scattering, this is not necessarily true, and one obtains a number of points of constructive interference.

In explaining Bragg diffraction, we first must find a system of describing crystal structures. A crystal can be thought of as being composed of an infinite number of different atomic plane layers, each with a different spacing d and a different orientation. Bragg diffraction can occur from any plane of atoms, as long as equation 2 is satisfied.

Within a crystal lattice, atoms can be organized in many different ways, depending on their species–a given species of atom always packs in the same way, although a change of external conditions may cause this structure to change (Figure 1, (a)). The structure of the copper crystal used in this experiment is classified as being *body-centered cubic*. All cubic crystals have cubic unit cells where a_0, the unit cell size, is set by the length of one side.

In the more general case, the unit cell is defined by three vectors a, b, and c, each directed along unit cell edges and with magnitudes equal to the length of each side. Atomic planes are then classified according to *Miller indices*, (h, k, l), where h, k, and l are small integers and $a/h, k/b$, and l/c are the points where the plane intersects the three axes. (Figure 1, (b)). In this experiment, neutrons were diffracted from the (002) planes of copper.

4. TRANSMISSION CROSS SECTIONS

The transmission cross section for a given material is typically given in 10^{-24}cm^2, or barns, and can be expressed by the following equation:

$$\sigma = \frac{1}{M} ln \frac{I_0}{I} \tag{3}$$

here I = intensity of attenuated beam, I_0 = intensity of unattenuated beam, and T, the transmission, equals the ratio $\frac{I}{I_0}$, which is also equal to the ratio $\frac{N}{N_0}$, where N and N_0 are the number of particles in the attenuated and unattenuated beam, respectively.

$$\begin{aligned} M &= \text{areal density of nuclei} \\ &= \#\text{ of nuclei/cm}^2 \text{ sample} \\ &= \frac{A}{N_{Av}\rho x} \end{aligned} \tag{4}$$

where A is the atomic weight of the sample, N_{Av} is Avogadro's number, ρ is the density of the sample, and x is the thickness of the sample. The $1/v$ dependency of Boron's transmission cross section is given by $\sigma = (1.660 \times 10^{-22} cm^3/sec)(\frac{1}{v})$, and v is the velocity of neutrons given in meters/second (this relation calculated from graphs in [1].

5. EXPERIMENT

Figure 2 shows the experimental setup for the neutron velocity determinations. The collimated beam of thermal neutrons was directed down the runway by two fixed slots and was broken up into pulses of neutrons by the chopper disc, which spun at 240Hz. A BF_3 detector was used to detect the neutrons, chosen for its low efficiency so that the detector would display the 1/v dependency.

The neutrons were first allowed to impinge upon the BF_3 detector at the near distance while the Multi Channel Scanner (MCS) counted 100,000 passes over 128 time bins, where each time bin was 20μs long. Neutron events detected by the BF_3 detector were amplified before being

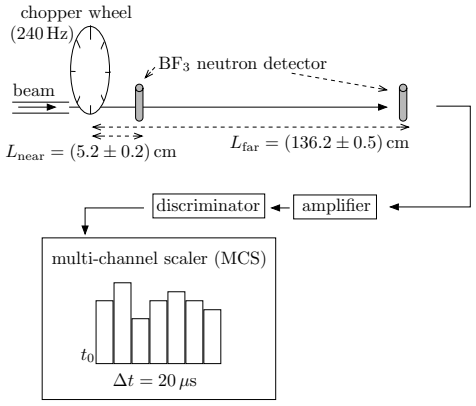

FIG. 2: Setup for determining neutrons' velocity. The detector is shown in near and far positions.

sent to a discriminator that distinguished between individual neutron impulses and sent its information to the Multi Channel Scaler. The MCS produced a histogram of the number of counts in time. At the start of a neutron burst, the slot detector senses that the slot in the chopper is lined up with the fixed slit. Then MCS begins counting neutron events and places all the counts from the first dwell in the first bin, then repeats the process for each successive bin. After it reaches the 128th bin, it stops counting until the next neutron burst begins, upon which it returns to the first bin and repeats the whole process.

The location of the highest build-up of neutron counts in the time channels (the peak of an approximately triangular distribution) of the MCS time display was then noted. Measurements with the detector at the far distance were made with the same MCS settings. and the peak times of the neutron build-up in the near and far position, C_{1p} and C_{2p} respectively, are used to obtain the time origin C_0 of the neutron beam. The neutron time origin channel must be calculated with a correction due to the finite flight time over the small distance the neutrons travel between the chopper wheel and the near location of the detector. The shape of the neutron burst in the MCS histogram is triangular, due to the fact that it represents the convolution of two rectangular areas– the moving slit on the chopper wheel and the fixed slit in the neutron beam runway. The channel spread of this triangular peak represents the limiting time resolution of the system.

To study Bragg diffraction, a copper crystal mounted on a goniometer was placed in the pathway of the neutron beam (Figure**??**). The copper crystal was rotated so that its (002) planes formed different θ_B with the beam of neutrons. Five different angles were chosen: $(15.0 \pm 0.1)^o, (17.5 \pm 0.1)^o, (20.0 \pm 0.1)^o, (22.5 \pm 0.1)^o, and (25.0 \pm 0.1^o)$ A high efficiency He detector was used in place of the BF_3 detector used before. The same measurement chain was used, and the MCS peak times of the neutron impulses were used to determine the velocities of the neutrons scattered by the crystal.

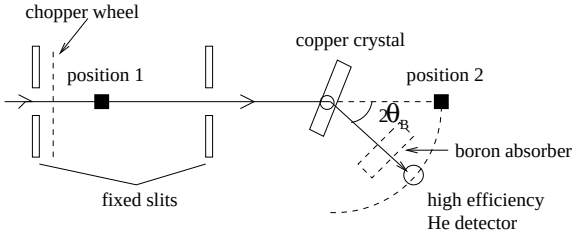

FIG. 3: Setup for Bragg diffraction and transmission cross section investigations.

To observe the transmission cross section of Boron, Pyrex, a boron-silicate glass, was placed between the diffracted neutron beam and the detector for four different values of θ_B: $(17.5 \pm 0.1)^o, (20.0 \pm 0.1)^o, (22.5 \pm 0.1)^o, and (25.0 \pm 0.1^0)$. The MCS gathered data for twice as many passes when the absorber was present, in order to obtain better resolution with the attenuated beam. The counts over the peak of the neutron beam were summed up with the absorber both absent and present in order to calculate the transmission T and the transmission cross section σ.

6. DATA AND ANALYSIS

Using the time spectroscopy data obtained in the first part of this experiment, the time origin C_0 of the neutron beam, which was calculated according to the following equation:

$$C_0 = C_{1p} - \frac{L_1}{(L_2 - L_1)}(C_{2p} - C_{1p}) \qquad (5)$$

where L_1 and L_2 are the near and far distances for the detector from the neutron chopper wheel. This time origin was used to calculate the velocities of the neutrons in the neutron beam, using the neutron peak times obtained from the Bragg diffraction measurements for different Bragg angles. The Bragg relation was then used to calculate the wavelengths of the neutrons.

In the transmission cross section measurements, the intensity in all channels over the peak of the MCS time spectral print-out was summed for the data with and without the absorber present, and the background subtracted from this sum. The background counts per time bin was obtained by summing over 20 non-peak bins and taking the average. The intensity measurements were then used to calculate Boron's transmission cross section. These values were then plotted against the values for $1/v$, where v was the velocity of the neutrons.

One source of systematic error in this experiment was the uncertainty in measuring the distance of the neutrons' flight from the reactor to the detector. Another systematic error was the uncertainty in determining the neutron peak location from the MCS printouts. Smoothing was used to make the location of the peak more evi-

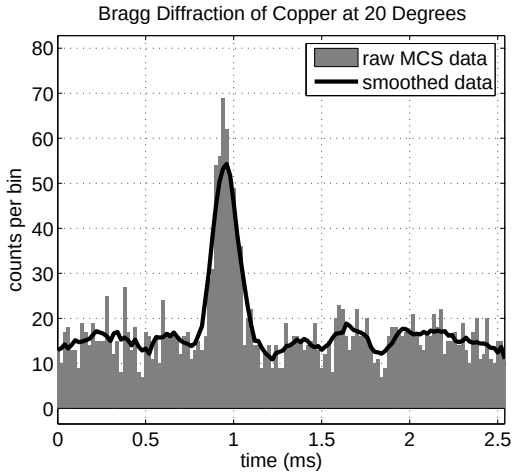

FIG. 4: Raw data and smoothed Bragg diffraction data for $\theta_B = (20.0 \pm 0.1)^o$. Smoothed data was obtained by using matlab to produce a plot where each point represented the average of the seven raw datapoints surrounding it. The smoothed curve was used in helping to determine the peak location and the spread of the peak.

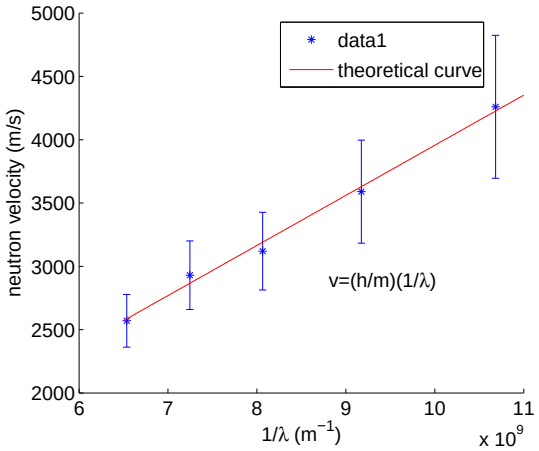

FIG. 5: Verification of the De Broglie relation using the Bragg diffraction data obtained in this experiment to calculate the velocity of the neutrons. Comparison to the theoretical line.

dent, but there was still uncertainty in the estimation of the peak's time.

One source of random error present in this experiment was the histogram error in the MCS printouts. Another was the fact that the measurements of neutron bursts may not have been recorded for sufficient amounts of time to obtain the proper resolution to draw an accurate picture of the phenomena, particularly in the case of the transmission cross section measurements, where the neutron beam was attenuated. Obtaining the background counts of neutron radiation may have also exhibited introduced random error, depending on whether or not there were smaller $\lambda/2$ diffraction effects that were not accounted for.

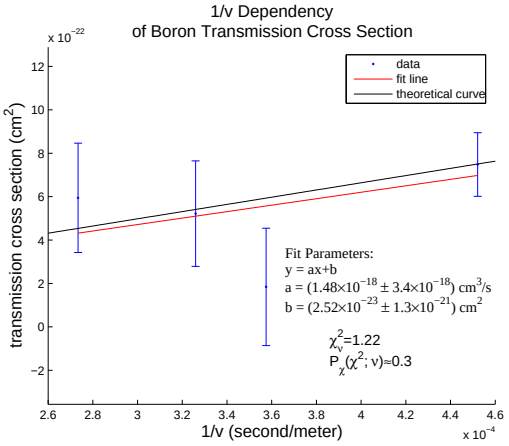

FIG. 6: Demonstration of the Boron transmission cross section's $\frac{1}{v}$ dependency.

7. CONCLUSIONS

For the Maxwell Boltzmann distribution fitting in the first part of this experiment, the temperature obtained for the reactor was $(64 \pm 19)^oC$, as compared to the actual reactor core temperature of 50.8^oC. The De Broglie relation was observed for neutrons, as evidenced by the close comparison of the experimental data to a plot of the theoretical relation. The experimental value obtained for the slope of the $1/v$ versus the transmission cross section of Boron was $(1.48 \times 10^{-18} \pm 3.4 \times 10^{-18}) cm^3/s$, while the theoretical value was $(1.660 \times 10^{-22} cm^3/sec)$. The theoretical value for the slope does fall within the range of the experimental data, and the fitted line compares well with the theoretical data, as seen in Figure 6, but the margin of error is large and even includes the possiblity of the slope being opposite in sign.

Improvements to this experiment might include studying more angles for the transmission cross section measurements. As this experiment only provided four points to fit to a line, it is not unexpected that there should be much uncertainty in the resulting fit parameters, as evidenced by the large standard deviation in both the slope and the intercept of the $\frac{1}{v}$ vs. σ plot. Future experiments could also involve investigating the transmission cross sections of other materials.

[1] J. L. Staff, *Junior Lab Reader* (Copytech, Fall 2004).
[2] J. D. McGervey, *Introduction to Modern Physics* (Academic Press, 1983).
[3] B. Rossi, *Optics* (Addison-Wesley, 1957).

Acknowledgments

The author wishes to acknowledge her fellow experimenter David Greenspan and the helpful Junior Lab Staff.